A MULTI-SCALE PERSPECTIVE OF TRMM-LBA CONVECTION

Robert Cifelli, Walter A. Petersen, Lawrence D. Carey, and Steven A. Rutledge
Department of Atmospheric Science
Colorado State University
Fort Collins, Colorado 80523

***Abstract*-This study presents an overview of Amazonian convection from the perspective of both ground and satellite intrumentation, with particular emphasis on radar observations of two MCSs that occurred during the TRMM-LBA field campaign. The MCSs formed in different meteorological regimes, based on profiles of atmospheric wind and thermodynamic data. The radar analyses show that the MCSs were distinct in terms of kinematic and microphysical characteristics. These observations suggest that the easterly and westerly wind regimes in the southwest Amazon region produce convection with different vertical structure characteristics, similar to regimes elsewhere in the global tropics (e.g., Maritime Continent).**

1. INTRODUCTION

Characterization of the vertical structure of convection and the corresponding latent heating distribution in tropical convection is a major objective of the NASA TRMM (Tropical Rainfall Measuring Mission) program. To support TRMM, a series of field campaigns were conducted in order to provide detailed information on tropical convection in various locations. One of these experiments, TRMM-LBA (Tropical Rainfall Measuring Mission – Large Scale Biosphere-Atmosphere Experiment in Amazonia), was conducted in the Amazon region in order to provide detailed information on precipitation characteristics in the interior of a tropical continent. TRMM-LBA was conducted in parallel with the WETAMC-LBA campaign aimed at examining the effect of land use change on rainfall in Amazonia.

II. METHODOLOGY

Details of the analysis method are presented in [1]. For our two cases, a total of 34 radar volumes were processed and analyzed (15 for 26 January and 19 for 25 February). The selected radar volumes spanned a continuous 2.5 hour period for the easterly event and 3 hour period for the westerly event at 10 minute temporal resolution. A partitioning algorithm based on [2] was used to separate areas of intense convection from weak convective-stratiform (WCSF) regions for each synthesized radar volume. A comparison of polarimetric radar-derived precipitation characteristics including precipitation ice mass and precipitation liquid water content were made using procedures similar to those outlined in [3]. As described in that paper, a difference reflectivity (Z_{dp}) method was used to discriminate horizontally polarized reflectivity (Z_H) for rain and ice.

III. METEOROLOGICAL REGIMES

On the global tropical scale, a three year analysis of TRMM-PR and LIS data suggest that wet-season convection in the Amazon is far from being "typical" of continental interiors. Distributions of the vertical radar reflectivity structure combined with LIS lightning flash densities place the Amazonian convection somewhere in the spectrum of convection ranging from that observed over isolated regions of tropical ocean, to the typically intense vertically developed convection of the African Congo [4].

On a more regional scale, the convection observed in the TRMM-LBA domain varied markedly in vertical structure as a function of the synoptic scale wind regime (Fig. 1). During extended periods of easterly wind at 850 mb, convection tended to take on more typical "continental" characteristics exhibiting deep vertical development and copious amounts of lightning. Conversely, during westerly periods in the 850 mb flow, the convection took on a much more "oceanic" characteristic, exhibiting a marked weakening in vertical structure and an overall reduction in lightning [1, 5, 6].

IV. RESULTS

A. General Characteristics of Convection

The 26 January MCS (Mesoscale Convective System) formed as a squall line with a leading line of convection and a trailing region of decaying convection and stratiform precipitation. The leading line was intense, with peak reflectivities exceeding 60 dBZ and echo tops approaching 19 km AGL. Peak updraft magnitudes were in excess of 20 m s^{-1}. The 25 February MCS was one of a number of westerly regime MCSs that were sampled during late February in TRMM-LBA. It's overall development appeared much more complex than the 26 January MCS. The storm organization could best be characterized as a broad area of relatively

homogeneous precipitation with apparently randomly oriented regions of embedded convection.

B. Composite Vertical Structure

Contoured Frequency by Altitude Diagrams (CFAD's) [7] and mean profiles of vertical air motion are shown in Fig. 2. Note that the modes of the distributions are nearly identical for the MCSs within each precipitation category. The major difference is the fact that the tails of the vertical draft distributions are significantly wider for the easterly MCS vs. the westerly MCS. That is, in the easterly case there is a higher relative frequency of occurrence of intense vertical velocity at all heights compared to the westerly case. The net effect of the differences at the tail of the distribution is to offset the magnitude of the mean profiles.

In the convective region, the mean vertical air motion profile (panel g of Fig. 2) for the easterly MCS has larger magnitude throughout the depth of the troposphere. Specifically, the mean easterly MCS profile is about 100% larger than the corresponding westerly profile below the melt level. The large drafts in the easterly MCS allow for a significant number of raindrops to be carried above the melt level and provide an important source of large ice particles and supercooled drops in this region, affecting the vertical distribution of hydrometeors in these MCSs.

In the WCSF region, the main difference in mean vertical air motion structure occurs below 8 km where the easterly MCS shows more low-level descent compared to the westerly profile (panel h of Fig. 2). The net effect of combining the WCSF and convective vertical air motion profiles (i.e., total category) is to reduce the magnitude of the easterly profile relative to the westerly MCS in the lower troposphere as well as to broaden the region of peak magnitude (panel i of Fig. 2).

Histograms of liquid and ice water content and mass weighted mean drop diameter in the mixed phase region (4-8 km) of the two MCSs are shown in Fig 3. This figure shows that the easterly MCS has a higher relative frequency of large ice and water drops in the mixed phase zone compared to the westerly event, which result in larger mean values of these quantities. Evidently, a significant portion of the rainwater mass in the westerly MCS was not lofted high and/or long enough to be converted into large precipitation ice as evidenced by the large difference in ice mass content between the two systems. Results shown in Fig. 3 suggest that ice microphysics probably played a more important role in rainfall production for the easterly MCS compared to the westerly MCS.

Results in Fig. 3 also indicate that the mean drop size (D_m) in the easterly MCS is larger compared to the westerly MCS. In fact, the offset in D_m is found to persist when all the S-pol radar data collected during TRMM-LBA are examined, suggesting different drop size distributions and corresponding Z-R relations for each regime [8]. These results are in agreement with surface disdrometer observations collected during TRMM-LBA. Figure 4 shows that the easterly MCS has a higher frequency of occurrence of intense rain rates compared to the westerly case, consistent with the higher ice water contents in the easterly event (Fig. 3). Similar differences in east vs west regime rain rate distributions have been observed from the TRMM PR [5] as well as in polarimteric-derived rainfall for the entire TRMM-LBA data set [8].

ACKNOWLEDGMENTS

This research was supported by NASA TRMM grant NAG5-4754. TRMM-LBA was supported by the NASA TRMM program under the direction of R. Kakar. Partial support for the S-Pol radar was provided by the National Science Foundation.

REFERENCES

[1] R. Cifelli, W.A. Petersen, L.D. Carey, and S.A. Rutledge, "Radar observations of the kinematic, microphysical, and precipitation characteristics of two MCSs in TRMM-LBA," unpublished.

[2] T.M. Rickenbach, and S.A. Rutledge, "Convection in TOGA COARE: Horizontal scale, morphology, and rainfall production," *J. Atmos. Sci*., vol. 55, pp. 2715-2729, 1998.

[3] L.D. Carey, S.A. Rutledge, D.A. Ahijevych, and T.D. Keenan, "Correcting propagation effects in C-band polarimetric radar observations of tropical convection using differential propagation phase," *J. Appl. Meteor*., vol. 39, pp. 1405-1433, 2000.

[4] W.A. Petersen, and S.A. Rutledge, "Regional variability in tropical convection: Observations from TRMM," *J. Climate*, in press.

[5] W.A. Petersen, S.W. Nesbitt, R.J. Blakeslee, R. Cifelli P. Hein, and S. A. Rutledge, "TRMM Observations of Convective Regimes in the Amazon, " unpublished.

[6] T.M. Rickenbach, R.N. Ferreira, J. Halverson, and M.A.F. Silva Dias, "Mesoscale properties of convection in western Amazonia in the context of large-scale wind regimes," unpublished.

[7] S.E. Yuter, and R.A. Houze, Jr., "Three-dimensional kinematic and microphysical evolution of Florida cumulonimbus. Part III: Vertical mass transport, mass divergence, and synthesis, " *Mon. Wea. Rev*., vol. 123, pp. 1964-1983, 1995.

[8] L.D. Carey, R. Cifelli, W.A. Petersen, S.A. Rutledge, and M.A.F. Silva Dias, "Characteristics of Amazonian rain measured during TRMM-LBA, " unpublished.

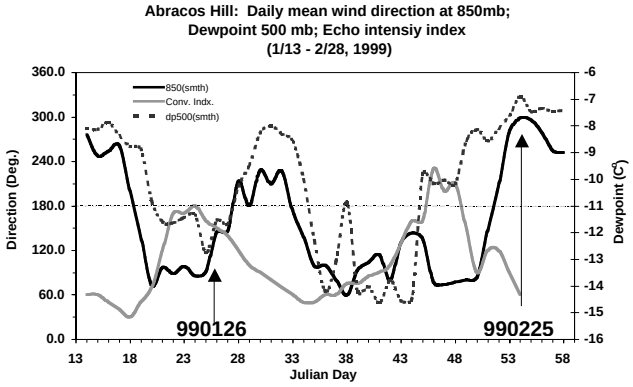

Figure 1. Time series of 850 mb smoothed wind direction (black solid line) and 500 mb dew point temperature (dashed line) from the Abracos Hill sounding site near the TOGA radar. The convective index (gray solid line) represents a ratio of total 40 dBZ area coverage / 10 dBZ area coverage using the TOGA radar data. A running mean has been applied to the time series. The time periods corresponding to the 26 January (990126) and 25 February (990225) MCSs are indicated.

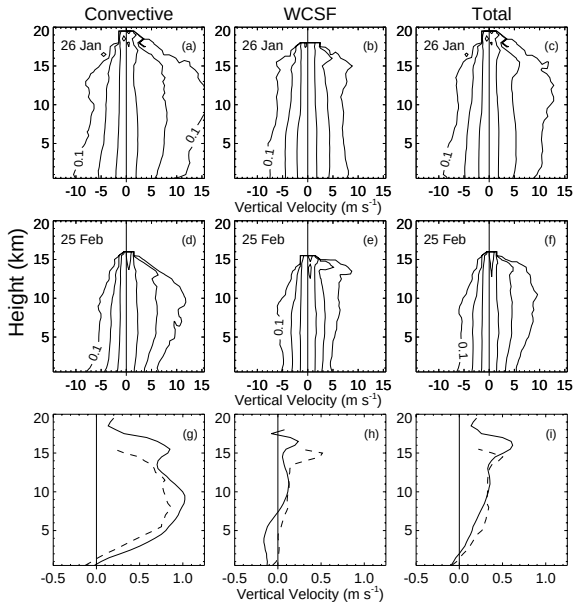

Figure 2. CFAD's of vertical air motion for the 26 January easterly (top row – panels a-c) and 25 February (middle row – panels d-f) events. Panels (g-1) are mean profiles for the 26 Janaury (solid line) and 25 February (dashed line) events. Panels from left to right in all rows are for convective, WCSF, and total (convective +WCSF) categories, respectively. CFAD contours are 0.1, 1.0, 10.0, and 30.0% relative frequency of occurrence. The CFAD's were constructed using a 1 m s^{-1} bin size and 31 total bins.

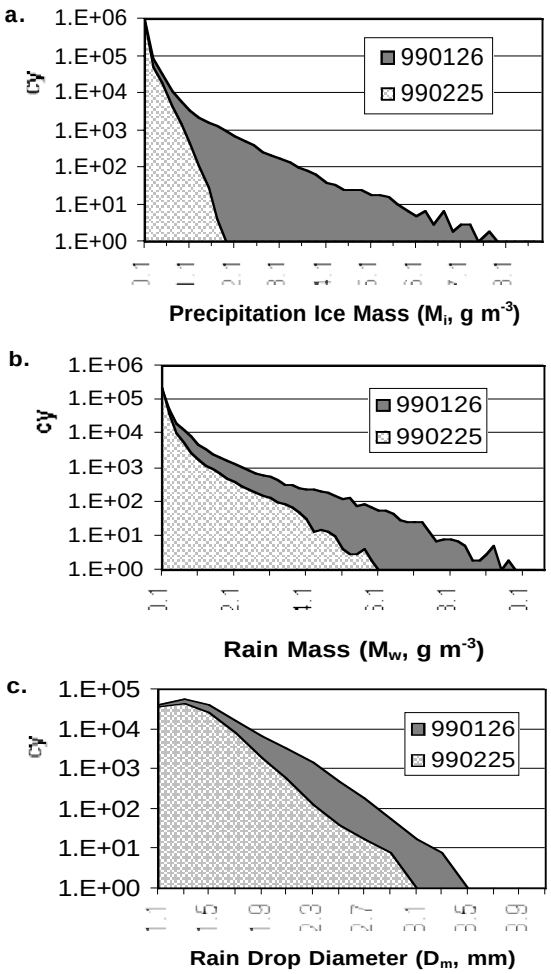

Figure 3. Frequency histograms of precipitation characteristics in the mixed phase zone (4-8 km) as derived from S-pol observations of horizontal and differential reflectivity. (a) Precipiation ice mass, (b) rain mass, and (c) mass weighted mean raindrop diameter.

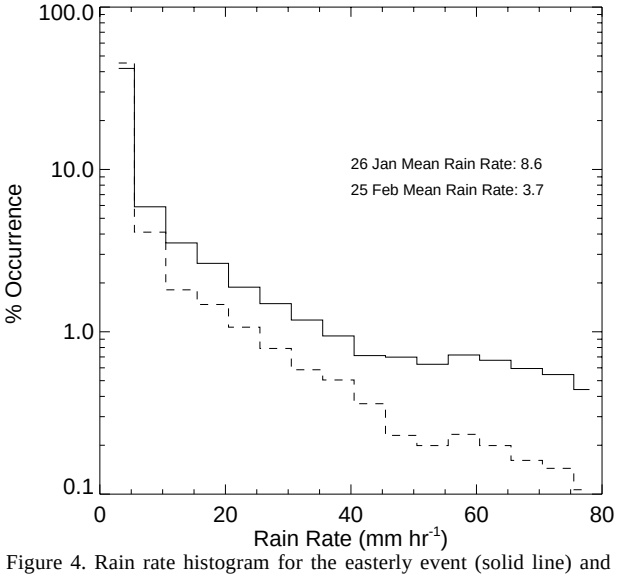

Figure 4. Rain rate histogram for the easterly event (solid line) and westerly event (dashed line).